Available online at http://scik.org

J. Math. Comput. Sci. 7 (2017), No. 3, 564-582

ISSN: 1927-5307

UNSTEADY BOUNDARY LAYER FLOW PAST A VERTICAL PLATE IN THE PRESENCE OF TRANSVERSE MAGNETIC FIELD AND HEAT SOURCE EMBEDDED IN A POROUS MEDIUM

M. SULEMANA[1,*], Y.I. SEINI[2], M.I. DAABO[1]

[1]Faculty of Mathematical Sciences,

University for Development Studies, Navrongo Campus, P. O. Box 1350, Tamale, Ghana

[2]School of Engineering,

University for Development Studies, Nyankpala Campus, P. O. Box 1350, Tamale, Ghana

Abstract: An investigation into the unsteady boundary layer flow past a vertical plate in the presence of transverse magnetic field and heat source embedded in a porous medium has been studied. The governing differential equation was transformed using suitable dimensionless parameters. The dimensionless equations were solved employing the Laplace transform techniques and results illustrated graphically for the velocity, temperature and concentration profiles as well as the Skin friction, Sherwood number and Nusselt number. The study concluded that all the controlling parameters had effects on the flow and can be used to control the flow kinematics.

Keywords: heat transfer; mass transfer; incompressible fluid; porous medium; Laplace transform.

2010 AMS Subject Classification: 35K05.

1. Introduction

Heat and mass transfer processes occur naturally in almost all physical phenomena. Indeed, no meaningful work can be done without the transfer of heat or mass. In many practical situations, heat and mass transfers depend on time resulting in unsteady processes. Unsteady boundary layer flow research has become important in recent times due to the several applications in industrial and engineering systems. It is commonly encountered in problems involving flow over helicopter

*Corresponding author

E-mail address: wunichee@yahoo.com

Received January 26, 2017; Published May 1, 2017

in translation motion, flow over blades of turbines and compressors, flow over the aerodynamic surfaces of vehicles in manned flight, start-up processes, periodic fluid motion and in the area of convective heat and mass transfers.

Unsteady boundary layer flow in the presence of magnetic field has applications in petroleum industries, geophysics, industrial and environmental processes, etc. In petroleum industries, it is applied in the exploration and thermal recovery of oil. In geophysics and astrophysics, its applications can be seen in the study of stellar and solar structures, radio-wave propagation etc. Industrial and environmental processes such as evaporation from open water reservoirs, heating and cooling processes, fossil fuel combustion and many other energy processes. Research in unsteady magnetohydrodynamics (MHD) through porous media is continuing due to its emerging industrial relevance.

Gupta *et al.* (1979) employed the perturbation method to investigate the free convection flow past a linearly accelerated vertical plate in the presence of viscous dissipation with Kafousias and Raptis (1981) extending it to include mass transfer effects subject to variable suction. Lesnic *et al.* (1999) studied the free convection boundary layer flow along a vertical surface in a porous medium with Newtonian heating whilst Muthucumaraswamy and Janakiraman (2006) investigated the mass transfer effects on exponentially accelerated isothermal vertical plate.Chaudhary *et al*. (2006) studied the unsteady free convection boundary-layer flow past an impulsively started vertical surface with Newtonian heating using the Laplace transform techniques and observed that the increase of Prandtl number results in decrease in temperature distribution.

Constatin et al. (2012) recently studied radiation and porosity effects on the magnetohydrodynamic flow past an oscillating vertical plate with uniform heat flux using Laplace transforms. It was observed that the radiation parameter reduces the temperature of the fluid. Bala *et al.* (2012) studied the radiation effects on MHD flow past an exponentially accelerated isothermal vertical plate embedded in porous medium in the presence of heat source and chemical reaction using Laplace transform methods. Their study established a direct correlation between the Grashof number, G_r and the velocity of the flow. Rout and Pattanayak (2013) extended the problem to include variable temperature embedded in a porous medium using Laplace transform techniques and observed that the temperature of the fluid increases with increasing radiation parameters. Seini (2013) studied the flow over an unsteady stretching surface with chemical reaction and non-uniform heat source using the Runge–Kutta–Fehlberg method with the shooting techniques and observed that heat and mass transfer rates as well as the skin friction coefficient increased as the unsteadiness parameter increases and decreased as the space-dependent and temperature-dependent parameters for heat source/sink increased.

Seini and Makinde (2013) studied MHD boundary layer flow due to exponential stretching surface with radiation and chemical reaction. A nonlinear velocity term with MHD was present in the temperature equation. It was found that the rate of heat transfer at the surface decreases with increasing values of the transverse magnetic field and the radiation parameter.

Ali et al. (2014) studied heat transfer boundary layer flow past an inclined stretching sheet in presence of magnetic field. A nonlinear velocity term with MHD was present in the temperature equation. It was found that velocity profile decreases due to increase of magnetic parameter, Prandtl number and Eckert number whilst velocity increases for increasing values of Grashof number.

Chamkha *et al*. (2014) analyzed the unsteady MHD free convection flow past an exponentially accelerated vertical plate with mass transfer. Arthur *et al*. (2015) investigated the MHD convective boundary layer flow towards a vertical surface in a porous medium with radiation, chemical reaction and internal heat generation using the Newton Raphson shooting method alongside the Fourth-order Runge - Kutta algorithm and concluded that the magnetic parameter an32d all the controlling parameters identified directly influence the flow around the boundary and hence can be controlled to achieve desired product characteristics.

Hussanan et. al. (2014) studied unsteady boundary layer flow and heat transfer of a Casson fluid past an oscillating vertical plate with Newtonian heating using laplace transform technique. It was observed that velocity decreases as casson parameters incresse and the thermal boundary layer thickness increases with increasing Newtonian heating parameter.

Hussanan et al. (2015) also investigated Soret effects on unsteady MHD mixed convective heat and mass transfer flow in a porous medium with Newtonian heating using Laplace transform technique and observed that the fluid velocity and the concentration increase with increasing values of soret number.

Hussanan et al. (2016) studied heat and mass transfer in a micropolar fluid with Newtonian heating. The plate executes cosine type oscillations. Exact solutions were obtained using Laplace transform technique.

To the best knowledge of the author, the unsteady boundary layer flow past a vertical plate in the presence of transverse magnetic field and heat source embedded in porous medium has not been documented. This study therefore attempts to investigate the problem using Laplace transform techniques.

2. Problem Formulation

Consider the unsteady boundary layer flow past a vertical plate in the presence of transverse magnetic field and heat source embedded in a porous medium. A magnetic field of uniform strength B_0 is applied transversely to the plate. Assuming the induced magnetic field produced by the motion of the electrically conducting fluid is negligible. The Reynolds number is also assumed to be very small since the induced magnetic field is negligible. The viscous dissipation is further assumed to be negligible. The flow is assumed to be in the $x^* - axis$ direction which is taken along the vertical plate in the upward direction. The y^* −axis is taken to be normal to the plate. The temperature of the plate and the ambient fluid are $T_w^*(x)$ and T_∞^* respectively. Initially, the plate and the fluid are at the same temperature T_∞^* with concentration level C_∞^* at all points. At time $t^* > 0$, the plate is exponentially accelerated with a velocity $u = U_0 e^{a^* t^*}$ in its own plane and the plate temperature is raised linearly with time t and the level of concentration near the plate is raised to C_w^*. The fluid under consideration is gray gas which absorbs or emits heat. The physical properties of the fluid such as the viscosity and thermal conductivity are assumed constant, while *Boussinesq* approximation invoked for the density variation in the body force term of the momentum equation. Under these assumptions, the boundary layer equations governing the unsteady flow process are:

$$\frac{\partial v^*}{\partial y^*} = 0 \tag{1}$$

$$\frac{\partial u^*}{\partial t^*} = \nu \frac{\partial^2 u^*}{\partial y^{*2}} + g\beta_T (T^* - T_\infty^*) + g\beta_C (C^* - C^*_\infty) - \frac{\sigma B_0^2}{\rho} u^* - \frac{\nu}{k^*} u^* \tag{2}$$

$$\frac{\partial T^*}{\partial t^*} = \alpha \frac{\partial^2 T^*}{\partial y^{*2}} - \frac{1}{\rho c_p} \frac{\partial q_r}{\partial y^*} - \frac{Q}{\rho c_p} (T^* - T^*_\infty) + \frac{\sigma B_0^2}{\rho c_p} u^{*2} \tag{3}$$

$$\frac{\partial C^*}{\partial t^*} = D \frac{\partial^2 C^*}{\partial y^{*2}} + D_1 \left(\frac{\partial^2 T^*}{\partial y^{*2}} \right) - K_C^* (C^* - C^*_\infty) \tag{4}$$

With boundary conditions

$$u^* = 0,\ T^* = T_\infty^* \qquad C^* = C_\infty^*\ for\ all\ y^*, t^* \leq 0$$
$$u* = U_0 e^{a*t*},\ T^* = T_\infty^* + (T_w^* - T_\infty^*)At*,\ C^* = C_w^*\ at\ y* = 0, t* > 0$$
$$u^* \to 0,\ T^* \to T_\infty^*,\ C^* \to C_\infty^*\ as\ y* \to \infty, t* > 0 \tag{5}$$

where u^* and v^* are the horizontal and vertical velocity components; U_0 is the velocity of the plate; y^* is the coordinate axis normal to the plate; t^* is time; v is the kinematic viscosity; β_T is the thermal expansion coefficient; β_C is the concentration expansion co-efficient; ρ is the fluid density; T^* is the fluid temperature near the plate; T_w^* is the fluid temperature at the plate surface; T_∞^* is the temperature of the free stream; C^* is the concentration in the fluid; C_∞^* is the concentration far away from the plate ; C_w^* is the concentration at the plate surface; a is the acceleration parameter ; D is the chemical molecular diffusivity; $\propto$ is the thermal diffusivity; C_p is the specific heat at constant pressure; K_c^* is the rate of chemical reaction; k* is the permeability co-efficient of the porous medium, q_r is the radiation heat flux, Q is the heat source parameter.

The following dimensionless variables and parameters as used in Rout and Pattanayak (2013) and Barik (2016) are introduced:

$$u = \frac{u*}{U_0},\ y = \frac{U_0 y*}{v}, Q = \frac{vQ_0}{U_0^2 \rho C_p}, \theta = \frac{T^* - T_\infty^*}{T_w^* - T_\infty^*},\ ,\ t = \frac{t^* U_0^2}{v},\ k = \frac{U_0^2 k^*}{v^2},$$
$$\emptyset = \frac{C^* - C_\infty^*}{C_w^* - C_\infty},\ P_r = \frac{\mu C_p}{k} \text{ or } P_r = \frac{v}{\propto},\ M = \frac{\sigma B_0^2 v}{\rho U_0^2},\ G_r = \frac{v\, g\beta_T (T_w^* - T_\infty^*)}{U_0^3},\ G_C = \frac{v\, g\beta_c (C_w^* - C_\infty^*)}{U_0^3},$$
$$k_c = \frac{v\, k_c^*}{U_0^2},\ S_0 = \frac{D_1 (T_w^* - T_\infty^*)}{v\, (C_w^* - C_\infty^*)},\ H = \frac{Qv^2}{kU_0^2},\ a = \frac{a^* v}{U_0^2},\ A = \frac{U_0^2}{v}, F = \frac{16\sigma a^* v^2 T_\infty^{*3}}{KU_0^2}$$
$$E_c = \frac{u^2}{C_p (T_w^* - T_\infty^*)} \tag{6}$$

where y is dimensionless coordinate axis normal to the plate surface; u is the dimensionless velocity in x direction; θ is the dimensionless temperature; t is dimensionless time; k is dimensionless permeability of porous medium ; F is the radiation parameter; M is the magnetic parameter; H is the heat absorption parameter; A is a constant; B_0 is the uniform external magnetic field; μ is the dynamic viscosity; S_0 is the Soret number; S_c is the Schmidt number; P_r is the Prandtl number; Gr is the thermal Grashof number; Gc is the mass Grashof number; Q is the heat source parameter; σ is the electrical conductivity; $\emptyset$ is the dimensionless concentration in the fluid; g is the acceleration due to gravity; K is the thermal conductivity of the fluid; K_C is dimensionless rate of chemical reaction; E_c is the Eckert number

Using the Rosseland approximation

$$\frac{\partial q_r}{\partial y^*} = -4a^*\sigma(T_\infty^{*4} - T^{*4}) \tag{7}$$

where a^* =Rosseland mean absorption co-efficient, σ =Stefan-Boltzmann constant and q_r = radiative heat flux.

Assuming that the temperature differences with the flow are sufficiently small such that T^{*4} is expressed as a linear function of the temperature. By Taylor series expansion and neglecting the higher order terms, T^{*4} is expressed as a linear function of the temperature in the form

$$T^{*4} \approx 4T_\infty^{*3}T^* - 3T_\infty^{*4} \tag{8}$$

Substituting (8) into (7) results in

$$\frac{\partial q_r}{\partial y^*} = -16a^*\sigma T_\infty^{*3}(T_\infty^* - T^*) \tag{9}$$

Using (6) and (9), equations (2) to (4) are reduced to:

$$\frac{\partial u}{\partial t} = \frac{\partial^2 u}{\partial y^2} + Gr\theta + G_c\emptyset - M_1 u \tag{10}$$

where $M_1 = M + \frac{1}{K}$

$$\frac{\partial \theta}{\partial t} = \frac{1}{\Pr}\frac{\partial^2 \theta}{\partial y^2} - \frac{1}{P_r}F_1\theta + ME_c u^2 \tag{11}$$

where $F_1 = F + H$,

$$\frac{\partial \phi}{\partial t} = \frac{1}{Sc}\frac{\partial^2 \phi}{\partial y^2} + So\frac{\partial^2 \theta}{\partial y^2} - Kc\phi \tag{12}$$

With the boundary conditions

$$u = 0, \theta = 0, \emptyset = 0 \quad for\ all \quad y, t \leq 0$$

$$u = e^{at}, \theta = 1, \emptyset = 1 \quad at \quad y = 0, t > 0$$

$$u \to 0, \theta \to 0, \emptyset \to 0 \quad as \quad y \to \infty, t > 0 \tag{13}$$

3. Problem Solution

The non-linear differential equations (10) to (12) with boundary conditions (13) are solved in exact form using the Laplace transform techniques:

The Laplace transforms of (10) to (12) and the boundary conditions (13) are as follow:

Thus, $\boldsymbol{\theta}(\boldsymbol{y}, \boldsymbol{s})=\left(1 + \frac{1}{P_r}F_1\frac{1}{s} - \frac{ME_c\left(e^{at}\right)^2}{s}\right)e^{-\sqrt{sP_r}\,y} - \frac{1}{P_r}F_1\frac{1}{s} + \frac{ME_c\left(e^{at}\right)^2}{s}$

$$= e^{-\sqrt{sP_r}\,y} + \frac{1}{P_r}F_1\left(\frac{1}{s}e^{-\sqrt{sP_r}\,y} - \frac{1}{s}\right) + ME_c(e^{at})^2\left(\frac{1}{s} - \frac{1}{s}e^{-\sqrt{sP_r}\,y}\right) \quad (14)$$

Taking inverse Laplace transforms. The general solution becomes

$$\boldsymbol{\theta}(\boldsymbol{y},\boldsymbol{t}) = \frac{y\sqrt{P_r}\; e^{-y^2P_r/4(t)}}{2\sqrt{\pi t^3}} + \frac{1}{P_r}F_1\left(1 - erf\left(\frac{y\sqrt{P_r}}{2\sqrt{t}}\right) - 1\right) + ME_c(e^{at})^2\left(1 - 1 + erf\left(\frac{y\sqrt{P_r}}{2\sqrt{t}}\right)\right)$$

$$= \frac{y\sqrt{P_r}\; e^{-y^2P_r/4(t)}}{2\sqrt{\pi t^3}} + \frac{1}{P_r}F_1\left(-erf\left(\frac{y\sqrt{P_r}}{2\sqrt{t}}\right)\right) + ME_c(e^{at})^2\left(erf\left(\frac{y\sqrt{P_r}}{2\sqrt{t}}\right)\right) \quad (15)$$

Where $F_1 = F + H$

Similarly, taking out the term $S_o\frac{\partial^2\theta}{\partial y^2}$ from the dimensionless concentration equation (12), where

$$\boldsymbol{\theta}(\boldsymbol{y},\boldsymbol{t}) = \frac{y\sqrt{P_r}\; e^{-y^2P_r/4(t)}}{2\sqrt{\pi t^3}} - \frac{1}{P_r}F_1\left(erf\left(\frac{y\sqrt{P_r}}{2\sqrt{t}}\right)\right) + ME_c(e^{at})^2\left(erf\left(\frac{y\sqrt{P_r}}{2\sqrt{t}}\right)\right)$$

The remaining equation is $\frac{\partial\phi}{\partial t} = \frac{1}{Sc}\frac{\partial^2\phi}{\partial y^2} - Kc\phi$ (16)

Taking inverse Laplace Transform,

The general solution becomes

$$\emptyset(\mathbf{y},\mathbf{t}) = \frac{y\sqrt{S_c}\; e^{-y^2S_c/(4t)}}{2\sqrt{\pi t^3}} + K_c\left(-erf\left(\frac{y\sqrt{S_c}}{2\sqrt{t}}\right)\right) \quad (17)$$

$$\emptyset(\mathbf{y},\mathbf{t}) = \frac{y\sqrt{S_c}\; e^{-y^2S_c/(4t)}}{2\sqrt{\pi t^3}} + K_c\left(-erf\left(\frac{y\sqrt{S_c}}{2\sqrt{t}}\right)\right) + S_o\left[\frac{y\sqrt{P_r}\; e^{-y^2P_r/4(t)}}{2\sqrt{\pi t^3}} - \frac{1}{P_r}F_1\left(erf\left(\frac{y\sqrt{P_r}}{2\sqrt{t}}\right)\right) + ME_c(e^{at})^2\left(erf\left(\frac{y\sqrt{P_r}}{2\sqrt{t}}\right)\right)\right] \quad (18)$$

Also, from the dimensionless momentum equation, we write

$$\frac{\partial^2 u}{\partial y^2} = \frac{\partial u}{\partial t} - Gr\theta - Gc\phi + M_1 u \quad (19)$$

The general solution is in the form:

$$\mathbf{U}(\mathbf{y},\mathbf{s}) = A(s)e^{-y\sqrt{s}} + B(s)e^{y\sqrt{s}} \quad (20)$$

Adding the term $G_r\theta\frac{1}{s} + G_c\emptyset\frac{1}{s} - M_1u\frac{1}{s}$ to (35) yields

$$\mathbf{U}(\mathbf{y},\mathbf{s}) = A(s)e^{-y\sqrt{s}} + B(s)e^{y\sqrt{s}} + G_r\theta\frac{1}{s} + G_c\emptyset\frac{1}{s} - M_1u\frac{1}{s} \quad (21)$$

Since $u(y,t) \to 0 \ as \quad y \to \infty, t > 0 \qquad \Rightarrow U(y,s) = 0$

From (34), $B(s) = 0$

Now (34) reduces to

$$\mathbf{U(y,s)} = A(s)e^{-y\sqrt{s}} + G_r\theta\frac{1}{s} + G_c\emptyset\frac{1}{s} - M_1 u\frac{1}{s} \qquad (22)$$

Since $u(0,t) = e^{at} \quad at \quad y = 0, t > 0 \qquad \Rightarrow u(0,s) = \frac{1}{s-a}$

Putting $A(s) = e^{at} - G_r\theta\frac{1}{s} - G_c\emptyset\frac{1}{s} + M_1 e^{at}\frac{1}{s}$ and $u(0,s) = e^{at}$ into (35)

$$\mathbf{U(y,s)} = \left(e^{at} - G_r\theta\frac{1}{s} - G_c\emptyset\frac{1}{s} + M_1 e^{at}\frac{1}{s}\right)e^{-y\sqrt{s}} + G_r\theta\frac{1}{s} + G_c\emptyset\frac{1}{s} - M_1 e^{at}\frac{1}{s} \qquad (23)$$

The general solution is

$$\boldsymbol{U(y,t)} = e^{at}\left(\frac{ye^{-y^2/(4t)}}{2\sqrt{\pi t^3}}\right) + G_r\theta\left(erf\left(\frac{y}{2\sqrt{t}}\right)\right) + G_c\emptyset\left(erf\left(\frac{y}{2\sqrt{t}}\right)\right) - M_1 e^{at}\left(erf\left(\frac{y}{2\sqrt{t}}\right)\right) \qquad (24)$$

Where $M_1 = M + \frac{1}{k}$,

$$\boldsymbol{\theta}(\mathbf{y},\mathbf{t}) = \frac{y\sqrt{P_r}\,e^{-y^2 P_r/4(t)}}{2\sqrt{\pi t^3}} - \frac{1}{P_r}F_1\left(erf\left(\frac{y\sqrt{P_r}}{2\sqrt{t}}\right)\right) + ME_c(e^{at})^2\left(erf\left(\frac{y\sqrt{P_r}}{2\sqrt{t}}\right)\right),$$

$$\emptyset(\mathbf{y},\mathbf{t}) = \frac{y\sqrt{S_c}\,e^{-y^2 S_c/(4t)}}{2\sqrt{\pi t^3}} + K_c\left(-erf\left(\frac{y\sqrt{S_c}}{2\sqrt{t}}\right)\right) + S_o\left[\frac{y\sqrt{P_r}\,e^{-y^2 P_r/4(t)}}{2\sqrt{\pi t^3}} + \frac{1}{P_r}F_1\left(-erf\left(\frac{y\sqrt{P_r}}{2\sqrt{t}}\right)\right) + ME_c(e^{at})^2\left(erf\left(\frac{y\sqrt{P_r}}{2\sqrt{t}}\right)\right)\right],$$

For the velocity profile, the general solution is

$$\boldsymbol{U(y,t)} = e^{at}\left(\frac{ye^{-y^2/(4t)}}{2\sqrt{\pi t^3}}\right) + G_r\left[\frac{y\sqrt{P_r}\,e^{-y^2 P_r/(4t)}}{2\sqrt{\pi t^3}} - \frac{1}{P_r}F_1\left(erf\left(\frac{y\sqrt{P_r}}{2\sqrt{t}}\right)\right) + ME_c(e^{at})^2\left(erf\left(\frac{y\sqrt{P_r}}{2\sqrt{t}}\right)\right)\right]\left(erf\left(\frac{y}{2\sqrt{t}}\right)\right) + G_c\left[\frac{y\sqrt{S_c}\,e^{-y^2 S_c/(4t)}}{2\sqrt{\pi t^3}} + K_c\left(-erf\left(\frac{y\sqrt{S_c}}{2\sqrt{t}}\right)\right) + S_o\left[\frac{y\sqrt{P_r}\,e^{-y^2 P_r/4(t)}}{2\sqrt{\pi t^3}} - \frac{1}{P_r}F_1\left(erf\left(\frac{y\sqrt{P_r}}{2\sqrt{t}}\right)\right) + ME_c(e^{at})^2\left(erf\left(\frac{y\sqrt{P_r}}{2\sqrt{t}}\right)\right)\right]\right]\left(erf\left(\frac{y}{2\sqrt{t}}\right)\right) + M_1 e^{at}\left(-erf\left(\frac{y}{2\sqrt{t}}\right)\right) \qquad (25)$$

Having obtained the temperature field, the rate of heat transfer coefficient at the vertical plate in terms of the Nusselt number can be studied. The effects of t, a, M, F, H, E_c and P_r on Nusselt number will be considered. In dimensionless form, the Nusselt number is given by

$$N_u = -\frac{\partial\theta}{\partial y}\bigg|_{y=0}$$

$$= -\frac{\sqrt{P_r}}{2\sqrt{\pi t^3}} + \frac{2}{\sqrt{\pi}}\frac{1}{P_r}F_1 - \frac{2}{\sqrt{\pi}}ME_c(e^{at})^2 \quad (26)$$

where $F_1 = F + H$

Knowing the concentration field, the rate of mass transfer coefficient at the vertical plate in terms of the Sherwood number can be studied. The effects of $t, a, M,\ F,\ H,\ S_c,\ P_r,\ E_c, S_0$ and K_c on Sherwood number will be examined. In dimensionless form, the Sherwood number is given by

$$sh = -\left(\frac{\partial \emptyset}{\partial y}\right)_{y=0}$$

$$= \frac{\sqrt{S_c}}{2\sqrt{\pi t^3}} - \frac{2}{\sqrt{\pi}}K_c + S_0\frac{\sqrt{P_r}}{2\sqrt{\pi t^3}} - \frac{2}{\sqrt{\pi}}\frac{1}{P_r}F_1 S_0 + \frac{2}{\sqrt{\pi}}ME_c(e^{at})^2 S_0 \quad (27)$$

Also, having obtained the velocity field, it is significant to study changes in the skin friction due to the effects of the physical parameters t, a, M and k. In dimensionless form, the skin friction is given by

$$\tau = \frac{\tau^*}{\rho U_0^2} = -\left.\frac{\partial u}{\partial y}\right|_{y=0} = \frac{1}{2\sqrt{\pi t^3}}e^{at} - \frac{2}{\sqrt{\pi}}M_1 e^{at} \quad (28)$$

where $M_1 = M + \frac{1}{k}$

4. Results and Discussion

In order to understand the physical dynamics of the problem, the effects of the controlling parameters on the Temperature (θ), Concentration$(\emptyset)$ and Velocity (u) profiles are illustrated graphically.

Fig. 1 illustrates the effects of Prandtl number (Pr) on the temperature profiles. Although smaller value of Pr means increasing of thermal conductivities which enables diffusion of more heat, however, when a magnetic field or MHD term is added to the energy equation the reverse process occur. It is therefore, observed that increasing the Prandtl number (Pr) increases the temperature of the fluid. Fig. 2 and 3 exhibit the effects of Heat absorption parameter (H) and Radiation Parameter (F) on the temperature profiles. It is observed that increase in either the Heat absorption parameter (H) or Radiation Parameter (F) decreases the temperature of the fluid flow. This is in good agreement with Rout and Pattanayak (2013) as well as Seini and Makinde (2013).

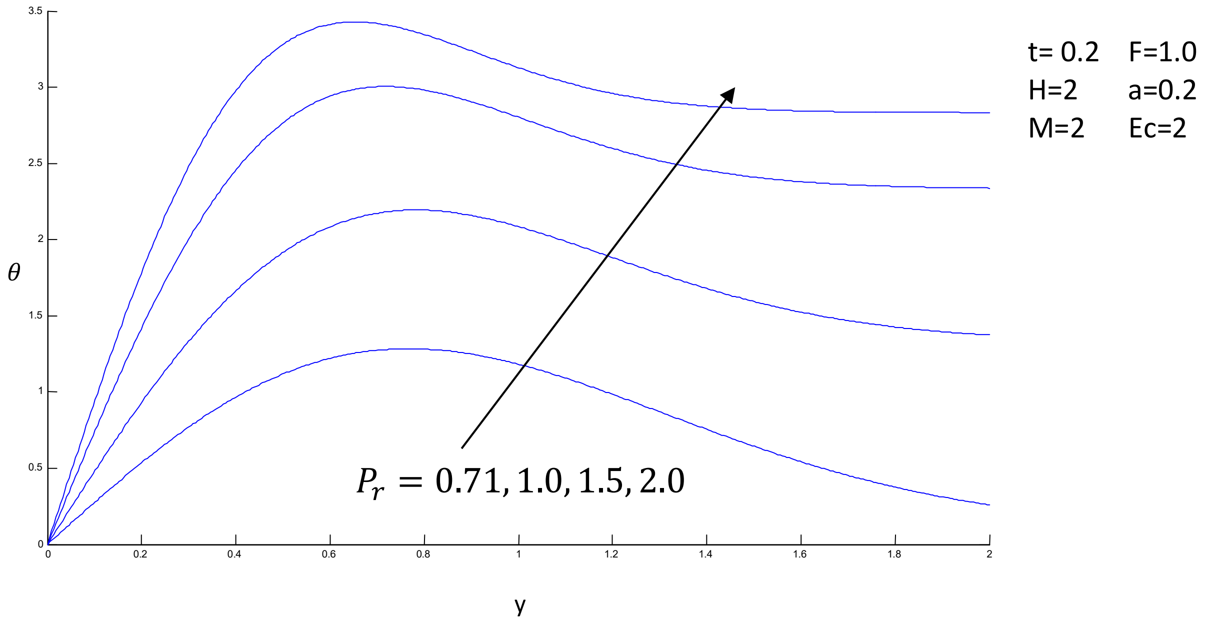

Fig. 1 Effects of Prandtl number (Pr) on the temperature profiles

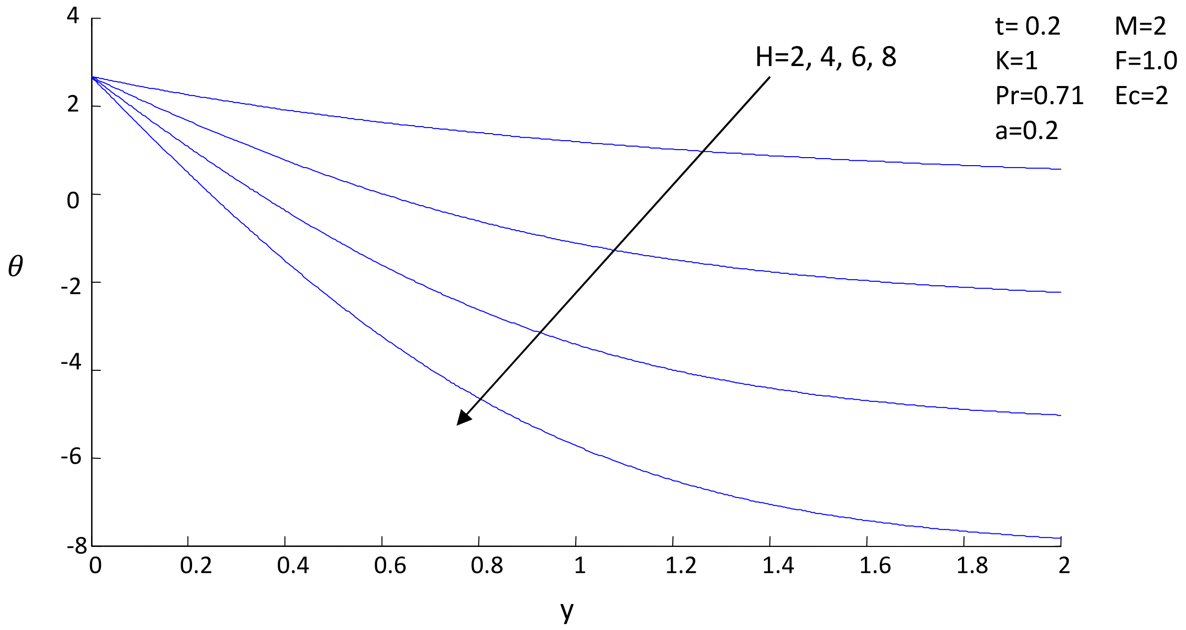

Figure 2. Effect of H (Heat absorption parameter) on the temperature profiles

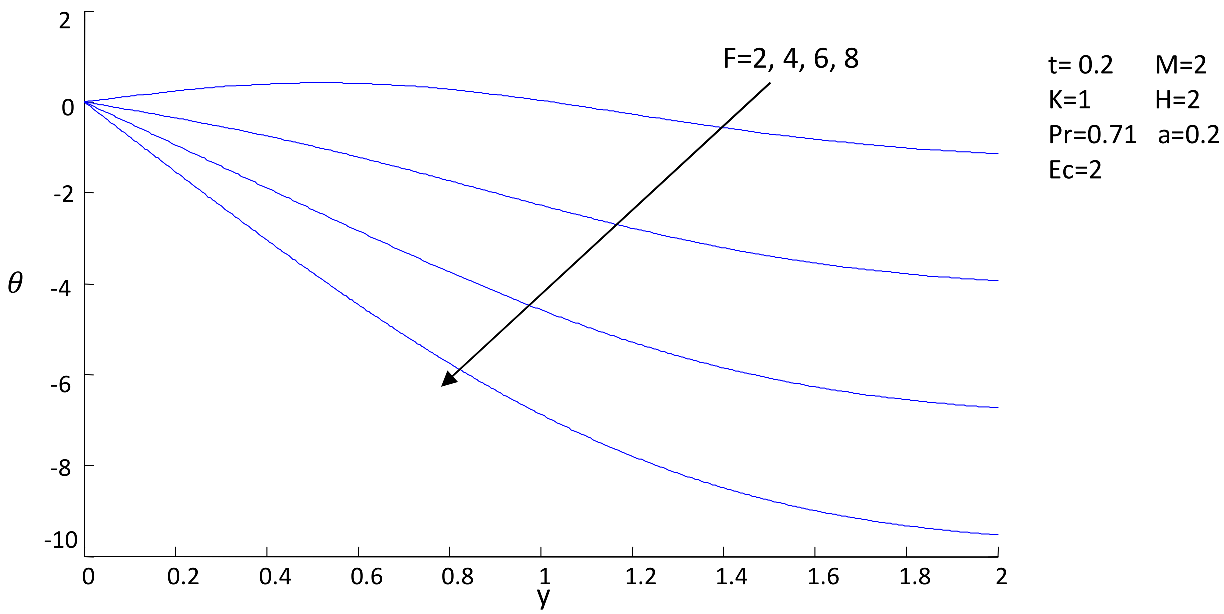

Figure 3. Effects of F (Radiation parameter) on the temperature profiles

Fig. 4 shows the effects of Chemical reaction parameter (Kc) on the concentration profiles. It is observed that an increase in the chemical reaction parameter, Kc decreases the concentration.

In Fig. 5 the effects of Soret number (S_0) on the concentration profiles is considered. It is observed that an increase in Soret number (S_o) increases the concentration of the flow. That is, it is observed that concentration distribution increases at all points of the flow field with increased in S_0 hence greater permeability of the porous medium.

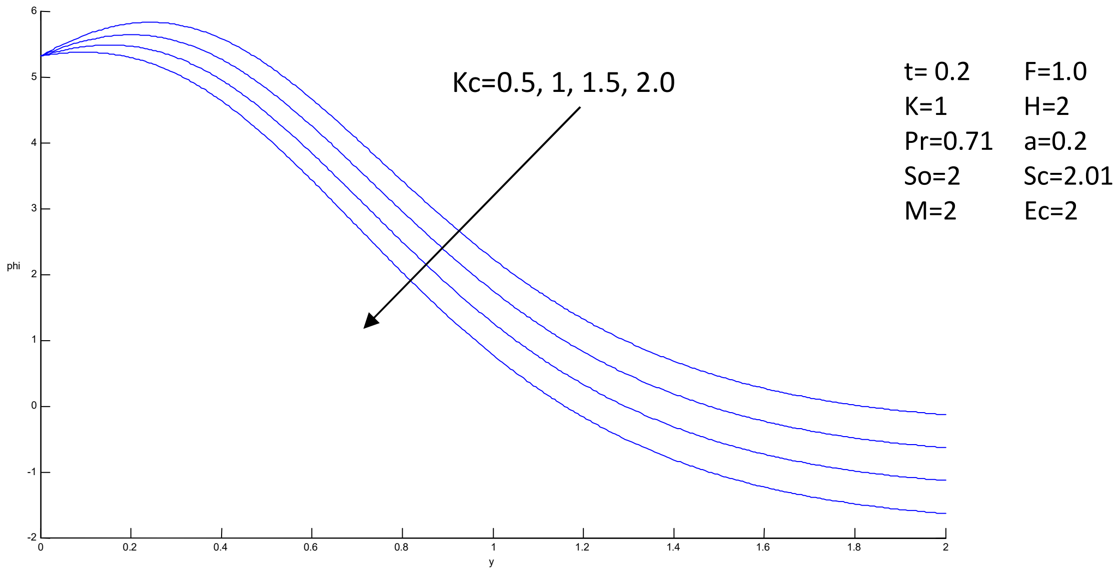

Fig. 4 Effects of K_C (Chemical reaction parameter) on the concentration profiles.

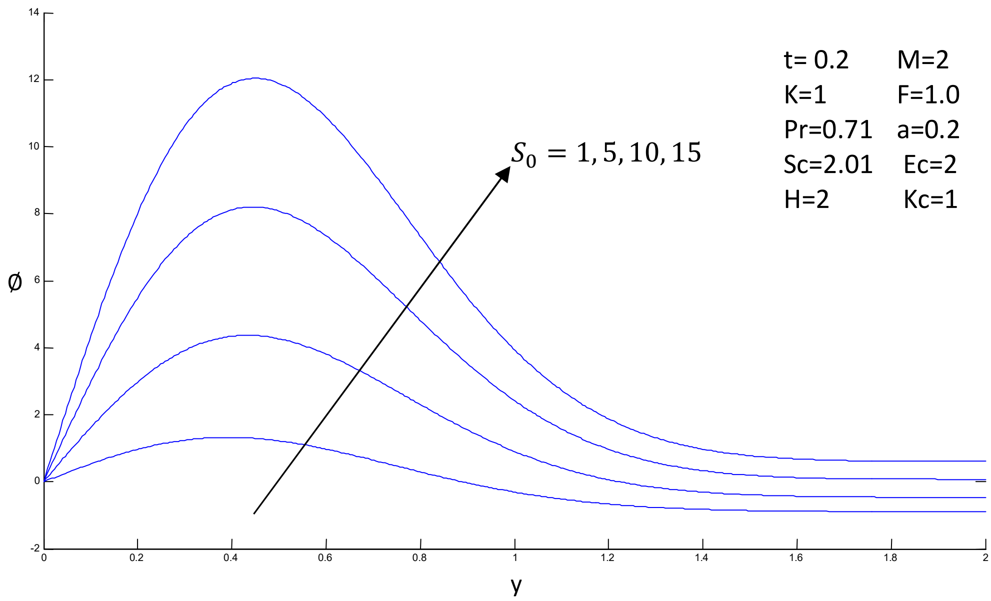

Fig. 5 Effects of Soret number (So) on the concentration profiles

Fig. 6, 7 and 8 illustrate the effects of Mass Grashof number Gc, Grashof number (Gr) and Schmidt number (Sc) on the velocity profiles respectively. It is observed that an increase in Gc leads to decrease in the velocity of the fluid flow whilst an increase in Gr or Sc leads to increase in the velocity of the flow as depicted in the diagrams which is in good agreement with Ali et al. (2014).

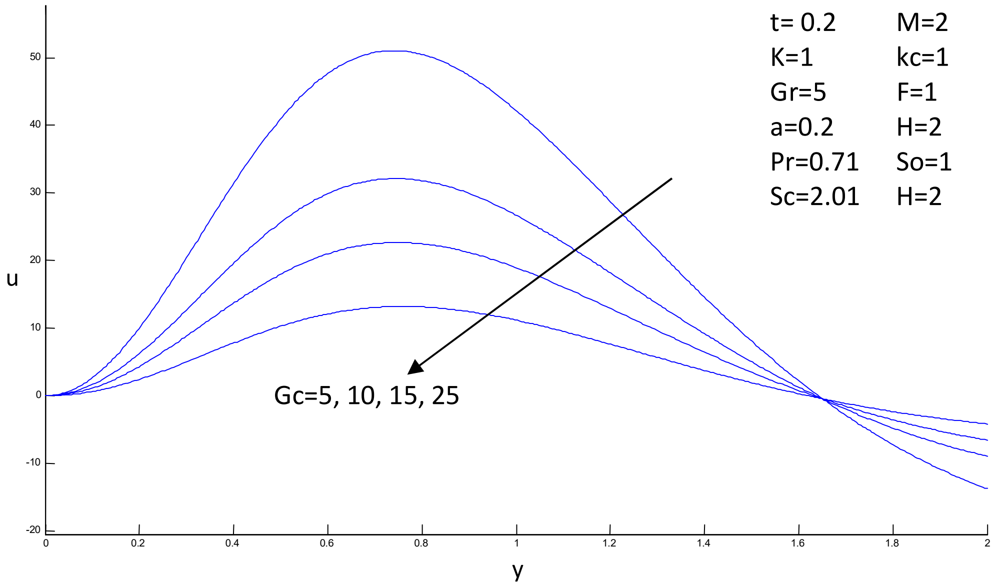

Fig. 6 Effects of Mass Grashof number (G_C) on the velocity profiles

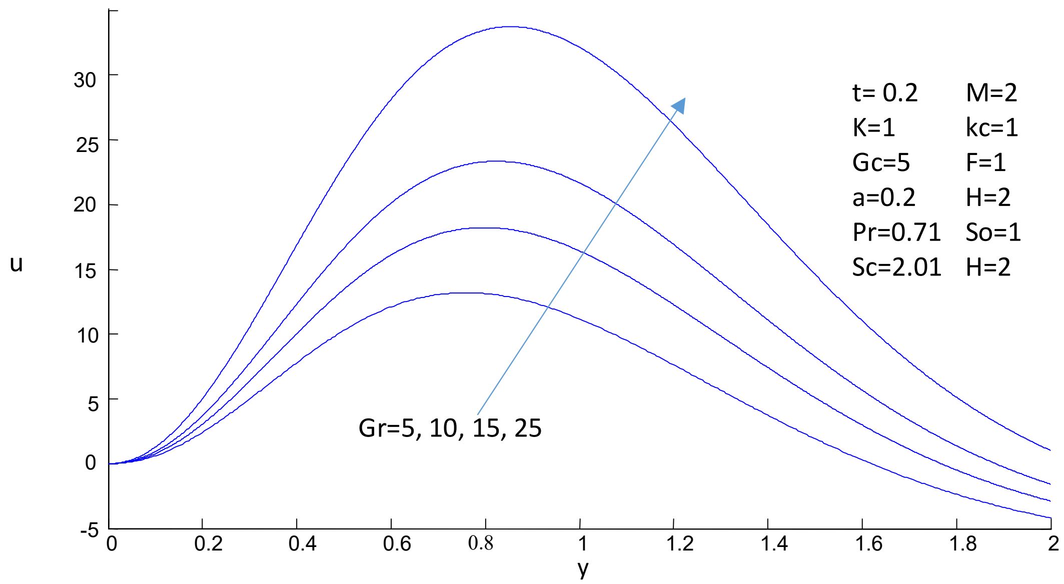

Fig. 7 Effects of Grashof number (Gr) on the velocity profiles

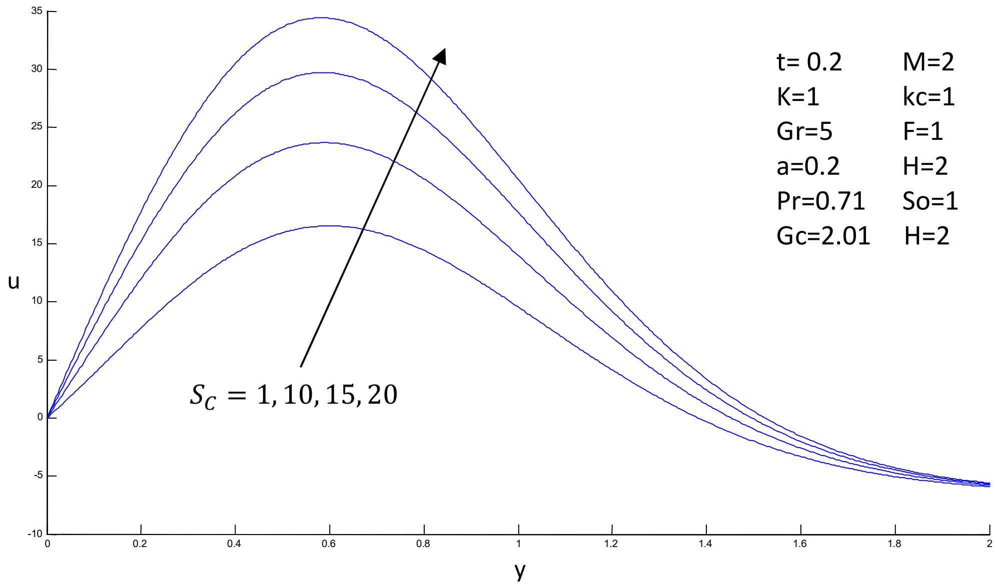

Fig. 8 Effects of Schmidt number (S_C) on the velocity profiles

Nusselt Number

Fig. 9 and 10 show the effects of Prandtl number (Pr) and Eckert number (Ec) on the Nusselt number profiles respectively. It is observed that increase in Pr leads to decrease in the Nusselt number whilst increase in Ec leads to increase in the Nusselt number.

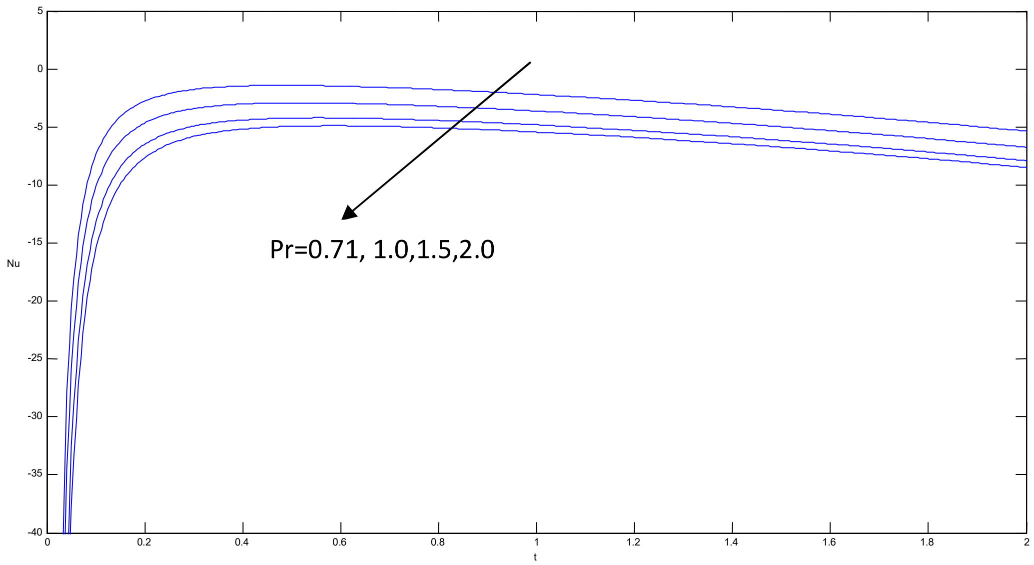

Fig. 9 The effects of Pr on the Nusselt number profiles

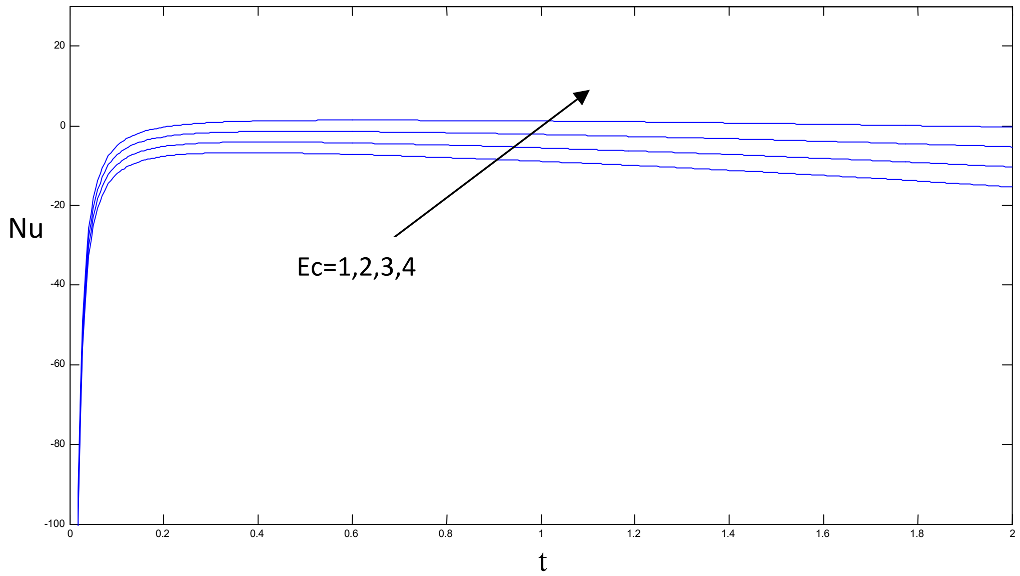

Fig. 10 The effects of Ec on the Nusselt number profiles

Sherwood Number

Fig. 11 and 12 show the effects of Schmidt number (Sc) and Heat absorption parameter (H) on the Sherwood number profiles respectively. It is observed that an increase in **Sc** results in increase in the Sherwood Number whilst increase in H decreases the Sherwood number.

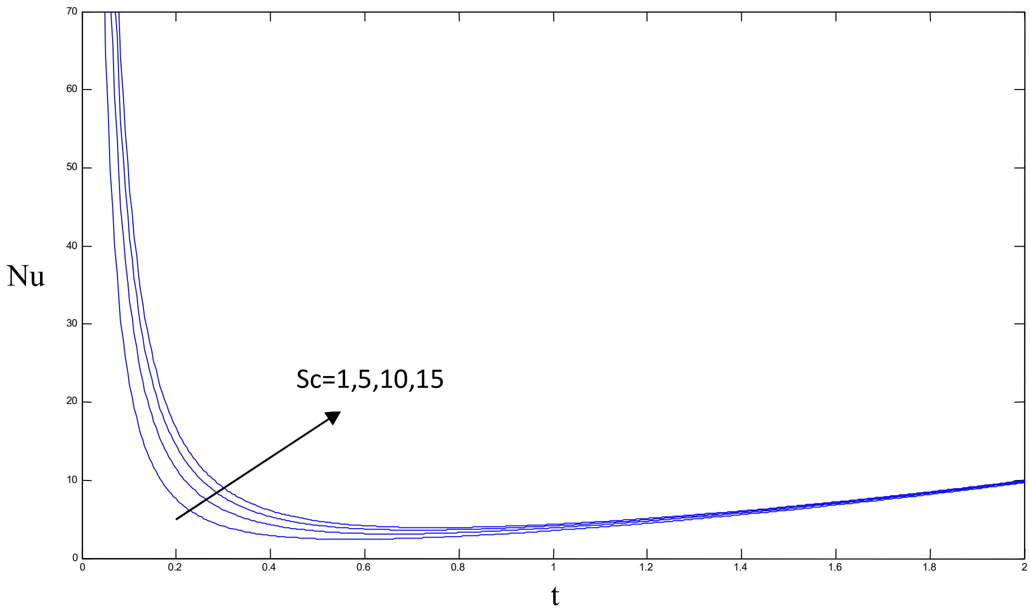

Fig. 11 Effects of Sc on the Sherwood number profiles

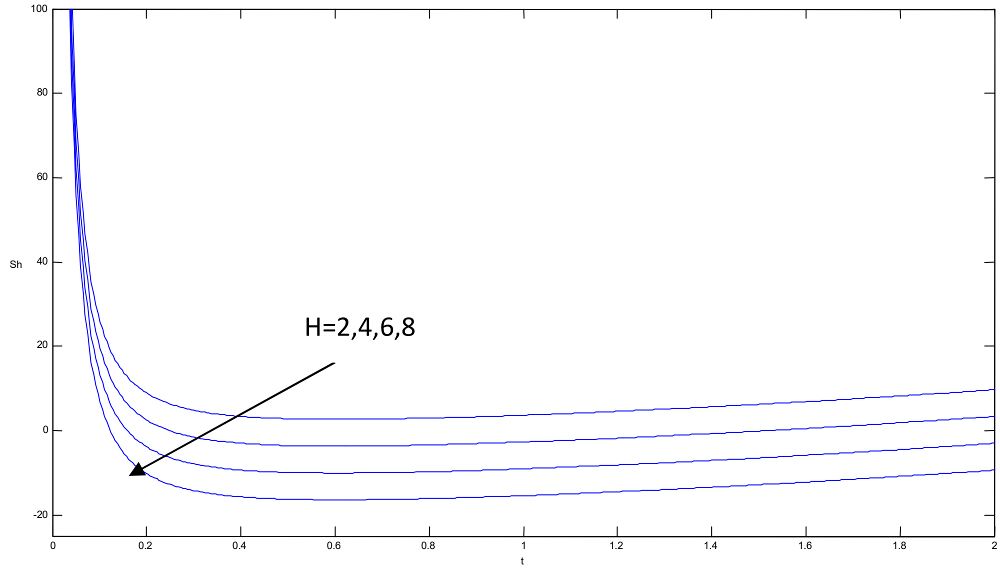

Fig. 12 Effects of H on the Sherwood number profiles

Skin Friction Fig. 13 and 14 show the effects of Magnetic parameter (M) and permeability of porous medium (K) on the Skin Friction coefficient respectively. It is noticed that an increase in M results in decrease in the Skin Friction coefficient whilst increase in K results in increase in the Skin Friction coefficient.

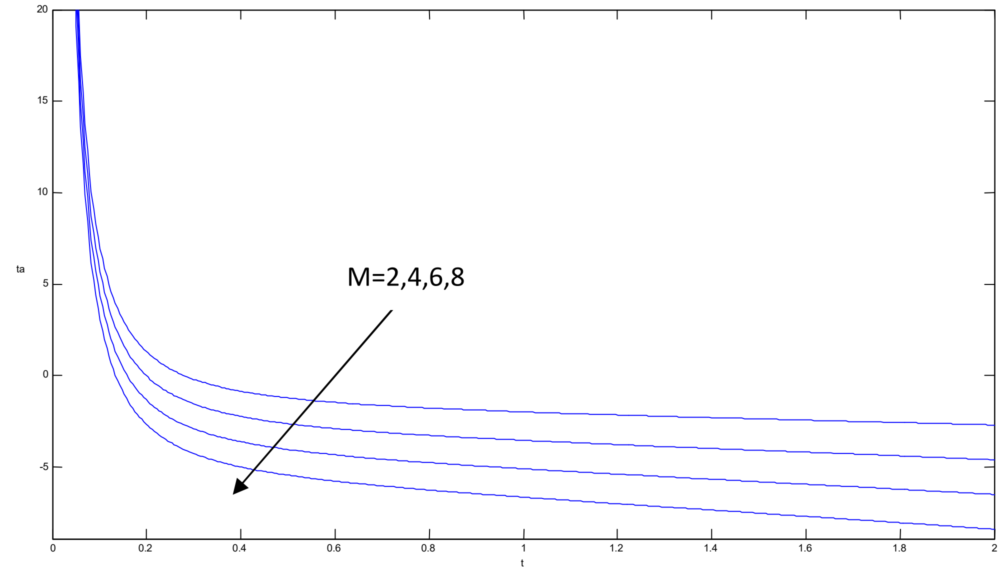

Fig. 13 Effects of M on the Skin Friction coefficient

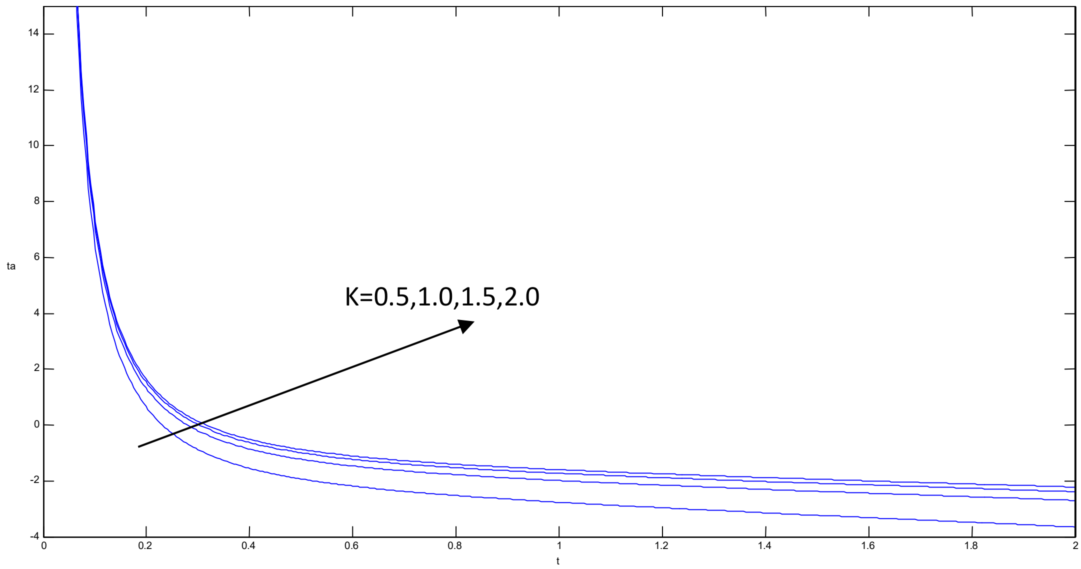

Fig. 14 Effects of K on the Skin Friction coefficient profiles

Conclusion

The MHD unsteady boundary layer flow in the presence heat generation in porous medium haven been investigated. The non-linear partial differential equations have been modeled and transformed to appropriate ordinary differential equations using similarity variables. The Laplace transform techniques were employed to solve the resulting ODE's directly and results illustrated graphically. From the results obtained, the following conclusions can be drawn:

1. The thermal boundary layer thickness diminishes with the heat absorption parameter (H) or radiation parameter (F) but increases with the Prandtl number (Pr).
2. The concentration boundary layer thickness increases with the Soret number (S_0) whilst the Chemical reaction parameter (K_c) causes a reduction in the species concentration in the fluid.
3. The velocity of flow decreases with increase in Mass Grashof number (Gc) but increases with an increase in Grashof number (Gr) and Schmidt number (Sc).
4. The Nusselt number decreases with increase in Prandtl number (Pr) but increases with increase in Eckert number (Ec).
5. The Sherwood number decreases with increase in Heat absorption parameter (H) but increases with increase in Schmidt number (Sc).
6. The Skin Friction coefficient decreases with increase in Magnetic parameter (M) but increases with increase in permeability of porous medium (K).

Conflicts of Interest

The authors declare that there is no conflict of interests.

REFERENCES

[1] Gupta, A.S, Pop, I. and Soundalgekar, V.G. Free convection flow past a linearly accelerated vertical plate on the presence of viscous dissipation heat. Rev. Roum. Sci. Techn.-Mec. Apl. 24 (1979), 561-568.

[2] Kafousias, N.G and Raptis, A.A. Mass transfer effects subject to variable suction or injection. Rev. Roum. Sci. Techn. Mec. Apl. 26 (1981), 11-22.

[3] Lesnic, D. Ingham D. B. and Pop I. Free convection boundary layer flow along a vertical surface in a porous medium with Newtonian heating, Int. J. Heat Mass Transfer, 42 (1999), 2621-2627

[4] Muthucumaraswamy, R. and Janakiraman, Mass transfer effects on exponentially accelerated isothermal vertical plate. Theoret. Aple. Mech. 33(1) (2006), 17-29.

[5] Bala, P.A.R., Bhaskar, N.R. and Suneetha S.. Effects on MHD flow past an exponentially accelerated isothermal vertical plate embedded in porous medium in the presence of heat source and chemical reaction, J. Appl. Fluid Mech. 5(3) (2012), 119-126

[6] Constantin F., Samiulhaq, Ilyas k., Fard A. and Sharidan S., Radiation and Porosity Effects on the Magnetohydrodynamic Flow Past an Oscillating Vertical Plate with Uniform Heat Flux, Z. Naturforsch. 67a (2012), 572 – 580.

[7] Rout, B.R. and Pattanayak, H.B. Chemical reaction and radiation effect on MHD flow past an exponentially accelerated vertical plate in the presence of heat source with variable temperature embedded in a porous medium, Mathematical Theory and Modeling 3(8) (2013), 18-25

[8] Seini Y. I. Flow over unsteady stretching surface with chemical reaction and non-uniform heat source. J. Eng. Manuf. Technol. 1 (2013) 24-35

[9] Seini Y. I. and Makinde O. D. (2013). MHD Boundary Layer Flow due to Exponential Stretching Surface with Radiation and Chemical Reaction, Math. Probl. Eng. 2013(2013), Article ID 163614.

[10] Mohammed Ali, M.D Abdul Alim and Mohammed Shah Alam, Heat transfer boundary layer flow past an inclined stretching sheet in the presence of magnetic field, Int. J. Adv. Res. Technol. 3 (5) (2014), 34-40.

[11] Chamkha, A.J., Raju, M.C., Sudhakar, R.T. and Varma S.V.K.. Unsteady MHD free convection flow past an exponentially accelerated vertical plate with mass. Int. J. Microscale Nanoscale Thermal 5(1) (2014), 59-75.

[12] Hussanan, A., Salleh, M.Z., Khan, I. and Tahar R.M. Unsteady boundary layer flow and heat transfer of a Casson fluid past an oscillating vertical plate with Newtonian heating. Plos One, 9(10) (2014), Article ID e108763.

[13] Arthur E. M., Ayando T. and Seini Y. I. MHD convective boundary layer flow towards a vertical surface in a porous medium with radiation, chemical reaction and internal heat generation. Frontiers in Heat and Mass Transfer (FHMT), 6 (2015), Article ID 21.

[14] Hussanan, A., Salleh, M.Z., Khan, I.Tahar R.M and Ismail, Z. Soret effects onunsteady MHD mixed convective heat and mass transfer flow in a porous medium with Newtonian heating. Maejo Int. J. Sci. Technol. 9(2) (2015), 224-245.

[15] Hussanan, A., Salleh, M.Z., Khan, I. and Tahar R.M. Heat and mass transfer in a micropolar fluid with Newtonian heating: an exact analysis. Neural Comput & Applic (2016). doi:10.1007/s00521-016-2516-0.

[16] Barik, R.N. Heat and mass transfer on unsteady MHD flow through an accelerated isothermal vertical plate embedded in porous medium in the presence of heat source and chemical reaction, Eur. J. Adv. Eng. Technol. 3(1) (2016), 56-61.

[17] Carslaw H.S and Jaeger J.C. Conduction of Heat in Solids (2nd edition), Oxford University Press, London, (1959).

[18] Abranmowitz B.M and Stegun I.A, Handbook of Mathematical Functions, Dover Publication, Inc. New York, (1970).

[19] Slattery J.C. Advanced Transport phenomena, Cambridge University Press, (1999).